Applied Physics Letters

Enhanced quantum dots spontaneous emission with metamaterial perfect absorbers

Cite as: Appl. Phys. Lett. **114**, 021103 (2019); https://doi.org/10.1063/1.5081688
Submitted: 15 November 2018 . Accepted: 03 January 2019 . Published Online: 15 January 2019

Wei Wang, Xiaodong Yang, Ting S. Luk, and Jie Gao

View Online Export Citation CrossMark

© 2019 Author(s).

Applied Physics Letters ARTICLE scitation.org/journal/apl

Enhanced quantum dots spontaneous emission with metamaterial perfect absorbers

Cite as: Appl. Phys. Lett. **114**, 021103 (2019); doi: 10.1063/1.5081688
Submitted: 15 November 2018 · Accepted: 03 January 2019 · Published Online: 15 January 2019

View Online Export Citation CrossMark

Wei Wang,[1] Xiaodong Yang,[1] Ting S. Luk,[2] and Jie Gao[1,a)]

AFFILIATIONS

[1] Department of Mechanical and Aerospace Engineering, Missouri University of Science and Technology, Rolla, Missouri 65409, USA
[2] Center for Integrated Nanotechnologies, Sandia National Laboratories, Albuquerque, New Mexico 87185, USA

[a)] Email: gaojie@mst.edu

ABSTRACT

Metamaterial perfect absorbers (PAs) made of a hexagonal array of holes on Ag-SiO_2-Ag thin films have been realized and utilized to enhance the spontaneous emission rate and photoluminescence intensity of CdSe/ZnS quantum dots (QDs) spin-coated on the absorber top surface. Perfect absorption of incoming light occurs at the wavelength where the impedance is matched to that of the free space. When QDs strongly excite both the electric and magnetic resonances at this perfect absorption wavelength, a significant Purcell effect on the spontaneous emission process and enhanced radiative outcoupling of photoluminescence intensity are expected. For perfect absorbers with near-unity absorption at the QD emission wavelength of 620 nm, 5-fold Purcell enhancement of the spontaneous emission rate and 3.6-fold enhancement of photoluminescence intensity are demonstrated in the time-resolved photoluminescence experiments, which are in good agreement with three-dimensional finite-difference time-domain simulation. These results will advance the understanding and applications of metamaterial PA-based light harvesting and emitting devices.

Published under license by AIP Publishing. https://doi.org/10.1063/1.5081688

Semiconductor quantum dot (QD) emitters are widely used in various photonic and optoelectronic applications such as light-emitting devices,[1] solar cells,[2,3] photodetectors,[4] nanolasers,[5] single-photon sources,[6] and photorefractive devices.[7,8] Enhancing the spontaneous emission rates of QDs is essential for the fundamental research of quantum electrodynamics[9] and also important for the advancements in single photon sources and low-threshold photonic and plasmonic lasers.[10] QD spontaneous emission can be manipulated by engineering the local density of optical states and the cavity Purcell effect.[11] Over the past few years, various optical nanostructures including nanocavities,[12–14] photonic crystals,[15–17] plasmonic nano-antennas,[18,19] and metamaterials[20–23] have been extensively studied for the enhancement of the spontaneous emission rate and the photoluminescence radiative efficiency. Recently, metamaterial perfect absorbers (PAs) have drawn much attention due to their capability to efficiently absorb light with subwavelength unit cells and have been widely used in many applications such as thermal photovoltaics,[24] thermal emitters,[25] sensors,[26,27] and color printing.[28–31] Perfect absorption arises from the presence of both electric resonance and magnetic resonance which results in the matched impedance to the free space. The impedance matched condition implies that the radiative damping and resistive damping are identical for the eigenmode in perfect absorber devices.[32,33] Coupling with perfect absorber eigenmodes which have equal resistive dissipation and radiative outcoupling, QD emitters will experience strong plasmon-exciton interactions and optimized radiative outcoupling at the desired wavelength, resulting in shortened QD photoluminescence decay lifetimes, large spontaneous emission Purcell factors, and enhanced far-field photoluminescence intensity.

In this letter, the enhancement of the spontaneous emission rate and photoluminescence intensity of CdSe/ZnS QDs coupled with metamaterial perfect absorbers was demonstrated. Metamaterial PAs made of a hexagonal array of holes on Ag-SiO_2-Ag thin layers with near-unity perfect absorption were realized, and the PA resonance wavelengths can be tuned across 200 nm in the visible wavelength range by changing the period and the hole radius of the unit cell structure. CdSe/ZnS QDs in the polystyrene thin layer were spin-coated on the surface of the metamaterial PAs. Time-resolved and spectral-resolved photoluminescence measurements were performed to characterize

Published under license by AIP Publishing

the spontaneous emission rate and photoluminescence intensity from the QD-PA devices. For the on-resonance PAs with high absorption at the QD emission wavelength, 5-fold Purcell enhancement of the spontaneous emission rate and 3.6-fold enhancement of photoluminescence intensity were observed. Numerical simulations of the emission rate and intensity enhancement, as well as the dipole-excited electric and magnetic field distributions, were carried out using the 3D finite-difference time-domain (FDTD) method, which agrees well with the experimental findings. This work not only has shown the enhanced QD spontaneous emission rates when the dipole emitters strongly couple to the on-resonance perfect absorbers but also has revealed that photoluminescence intensity enhancement is achieved at the same time due to the satisfied impedance match condition for the perfect absorber eigenmodes with balanced resistive dissipation and radiative outcoupling at the resonance wavelength. The results pave the way for the understanding of enhanced QD spontaneous emission and radiative outcoupling processes in the metamaterial perfect absorbers, also the advancement of metamaterial PA-based applications in light harvesting, light-emitting devices, solar cells, photodetectors, optical sensors, nano-scale lasers, and single-photon sources.

Figure 1(a) shows the three-dimensional schematic of metamaterial PAs with a hexagonal array of holes patterned on the top silver layer of the Ag-SiO_2-Ag three-layer structure. The bottom 100 nm Ag layer is deposited using an electron-beam evaporator system on top of a silicon wafer. The 45 nm SiO_2 spacer and the top 25 nm Ag layer are then deposited using the sputtering method (Kurt J. Lesker), where Ag is deposited at the rate of 0.4 Å/s and SiO_2 is deposited at 0.2 Å/s. The optical constant of both materials and the film thicknesses are characterized using variable angle spectroscopic ellipsometry (VASE, J. A. Woollam Co. VB400/HS-190). A layer of polystyrene mixed with CdSe/ZnS QDs[34] is spin-coated over the PA surface. A one-step Focused Ion Beam (FIB) milling (FEI Helios Nanolab 600 Dual Beam, 30 KV, 9.7 pA) is used to fabricate the nanostructures, and Fig. 1(b) presents the typical scanning electron microscopy (SEM) cross-sectional view of the PAs. By changing the structure period P and hole radius r, the PA resonance frequency can be tuned across the whole visible frequency region.[35] In order to match the QD emission wavelength at 620 nm, PA2 with period P of 230 nm and hole radius r of 65 nm is designed to be on-resonance with the QD emission, and the SEM image is shown in Fig. 1(d). Three other PAs with absorption resonances detuned from the QD emission wavelength are also designed and fabricated, and the SEM images are shown in Figs. 1(c), 1(e), and 1(f) with different lattice geometrical parameters (c: $P = 155$ nm, $r = 40$ nm; e: $P = 280$ nm, $r = 80$ nm; and f: $P = 315$ nm, $r = 90$ nm).

Reflectance spectra of the fabricated four metamaterial PAs are measured using a home-built microscope with a halogen lamp and a fiber-coupled spectrometer, and the plots are shown in Figs. 2(a)–2(d), respectively. Narrow resonances with nearly perfect absorption and very low reflectance are obtained at 524 nm, 618 nm, 683 nm, and 737 nm, respectively, for devices PA1, PA2, PA3, and PA4 covered with the QD layer. The gray shaded area (PL_0) in Fig. 2 represents the photoluminescence emission spectrum of CdSe/ZnS QDs centered on 620 nm. As depicted clearly, the absorption resonance in the reflectance spectrum of PA2 with a period of 230 nm and a radius of 65 nm matches with the QD emission wavelength perfectly with nearly perfect absorption ($A = 0.95$) and nearly zero reflectance ($R = 0.05$), while the resonance of PA1 (PA3) is blue-shifted (red-shifted) relative to the center of the QD emission and the absorption is 0.33 (0.35) at 620 nm. PA4 is largely off-resonance, and the absorption at the QD emission wavelength is very low

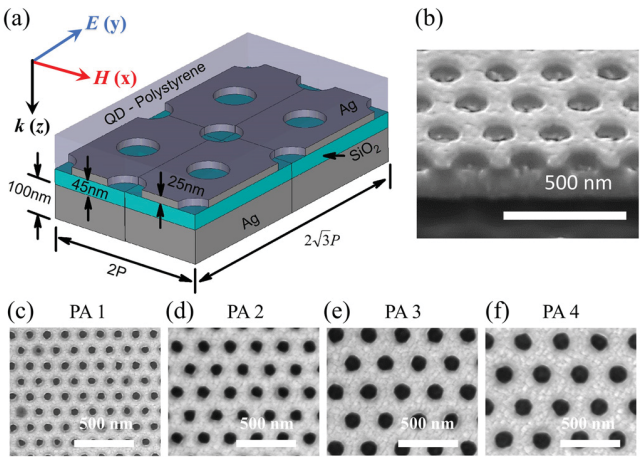

FIG. 1. (a) Schematic view of metamaterial PAs made of a hexagonal array of holes on the Ag-SiO_2-Ag three-layer structure with the spin-coated QD-polystyrene film. (b) SEM cross-section of metamaterial PA fabricated by FIB with a period of 230 nm and a hole radius of 65 nm. (c)–(f) SEM images of four structures with different lattice geometrical parameters (c: $P = 155$ nm, $r = 40$ nm; d: $P = 230$ nm, $r = 65$ nm; e: $P = 280$ nm, $r = 80$ nm; and f: $P = 315$ nm, $r = 90$ nm).

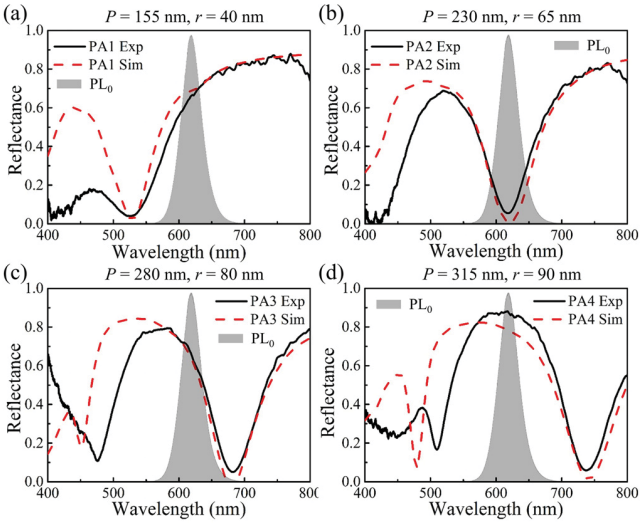

FIG. 2. Measured optical reflectance spectra of QD-polystyrene coated metamaterials PA1 (a), PA2 (b), PA3 (c), and PA4 (d) with different geometrical parameters as designed and fabricated in Fig. 1. The red dashed lines are the simulated reflectance spectra using the FDTD method.

Published under license by AIP Publishing

(A = 0.13). Notably, perfect absorption of incoming light in PA2 at 620 nm arises from the presence of both electric resonance and magnetic resonances, which results in the matched impedance to the free space.[33] Therefore, the coupling strength between QDs and the PA resonant mode, which plays an essential role in the QD emission process, is greatly enhanced. The on-resonance PA2 is expected to have the most significant Purcell effect which leads to the largest spontaneous emission rate among the four designed devices, as well as the maximum radiative outcoupling and photoluminescence intensity enhancement when working with the impedance matched condition. The red dashed lines in Fig. 2 are simulation results using the FDTD method, which agree very well with the measured resonance wavelengths and reflectance spectra.

To demonstrate the Purcell effect of the metamaterial perfect absorbers, time-resolved photoluminescence decay measurements of QDs on the PAs and the glass substrate (control) are carried out using a time-correlated single photon counting (TCSPC) system and a 402 nm picosecond pulsed laser with an excitation power of 0.25 μW. Figures 3(a)–3(d) show the photoluminescence decay data from QDs on the four PAs at an emission wavelength of 620 nm, where faster decays are observed on the four PAs than that on the glass substrate. It is also observed that the photoluminescence decay on PA2 is faster compared to that on other PAs, indicating a stronger Purcell effect of the on-resonance PA2 with nearly perfect absorption. The spontaneous emission decay lifetime of the QDs is obtained by fitting the experimental photoluminescence decay curves using a two-exponential relaxation model[20,22] and averaged from ten measurements for each PA design. For on-resonance PA2, the photoluminescence first decays with a shorter lifetime of t_1 ~4.28 ± 0.06 ns which is attributed to the QDs strongly coupled to the PA resonant mode and slows down to a longer lifetime of t_2 ~32.04 ± 0.97 ns which is determined mainly by those QDs away from the PA surface, whereas the QD decay on the glass substrate control sample shows a similar long lifetime of t_0 ~20.88 ± 0.01 ns. The shortened QD decay lifetimes on devices PA1, PA3, and PA4 are 4.77 ± 0.12 ns, 4.81 ± 0.09 ns, and 5.89 ± 0.11 ns, respectively. Figure 4(a) illustrates the emission rate enhancement of the four PAs, which is obtained by normalizing the QD decay lifetime t_0 on the glass substrate with the decay lifetime t_1 of QDs coupled to the PAs. Five-fold emission rate enhancement from PA2 is shown, which is the largest among the four devices. The strengthened coupling between the QDs and the PA resonant mode in PA2 with perfect absorption and impedance match at 620 nm contributes to the enhanced spontaneous emission rate in the measurement. For PA1 and PA3 with absorption of 0.33 and 0.35 at 620 nm, a similar level of emission rate enhancement (~4.3) is observed. However, small emission rate enhancement is reported for the most off-resonance PA4 due to the weak coupling strength between QDs and the PA mode in this device. The emission rate enhancement is also modeled using 3D FDTD simulation and averaged from electrical dipole emitters with three orthogonal polarizations and at 28 different positions (in the first quadrant due to symmetry) located 15 nm above the PA surface. The simulation results in Fig. 4(b) show excellent agreement with the experimental results for the comparison of QD emission rate enhancement on the four PAs.

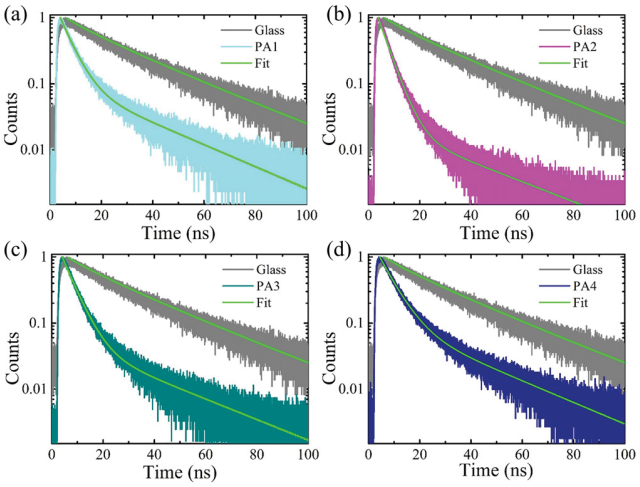

FIG. 3. Normalized TCSPC histograms and fitting results for QD photoluminescence decays on the four metamaterial PAs and the glass substrate.

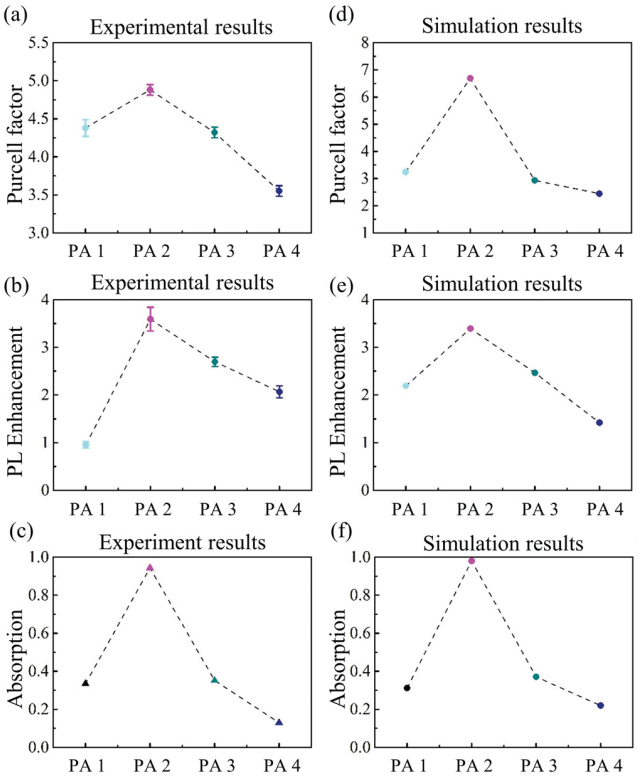

FIG. 4. Experimental and simulation results for spontaneous emission rate enhancement (a) and (b) and photoluminescence intensity enhancement (c) and (d) of the four metamaterial PAs coupled with QDs at 620 nm.

Published under license by AIP Publishing

In order to understand the enhancement effect on photoluminescence intensity radiated from the PAs, photoluminescence spectra of the four QD-PA devices are measured using a Horiba spectrometer and a liquid N_2 cooled CCD. Photoluminescence intensity from the four PAs at 620 nm is obtained, and the intensity enhancement is shown in Fig. 4(c) by normalizing to the QD photoluminescence intensity on the glass substrate. The on-resonance PA2 shows the largest photoluminescence intensity enhancement ~3.6 among the four devices, resulting from both the enhanced QD emission rate and the radiative outcoupling when QDs couple strongly with the PA resonant mode with the impedance matched condition. Simulation results of photoluminescence intensity collected within the collection angle of 33.4° (corresponds to the objective lens NA = 0.55 used in experiment) at a far-field plane from the PA surface normalized by that from the glass substrate are presented in Fig. 4(d), which also agrees with the observations in the experiment. It is worth mentioning that the general trend of spontaneous emission rate enhancement and photoluminescence intensity enhancement for the four PA devices is more or less the same with the trend of PA absorption, which suggests that the QD spontaneous emission process and the radiative outcoupling are greatly enhanced in the metamaterial PAs with high absorption and impedance match at the desired emission wavelength.

To show more clearly the excitation of the absorption resonances in the metamaterial PAs by QD emitters and the efficient outcoupling from the QD-PA devices, electric and magnetic field intensity distributions are illustrated in Fig. 5 with the excitation from an electric dipole emitter with the dipole moment along the vertical z direction and an emission wavelength of 620 nm. The top view cut at the middle of the top silver layer is shown in Figs. 5(a) and 5(c), and the side cross-sectional view is presented in Figs. 5(b) and 5(d). As expected, the dipole emission strongly excites the electric and magnetic resonances in PA2, and both the intensive electromagnetic resonant mode confinement and the strong radiative outcoupling contribute to the observed spontaneous emission rate enhancement and photoluminescence intensity enhancement in the experiment. Furthermore, simulations also show that placing QDs in the middle SiO_2 spacing layer at the locations of the electromagnetic field maxima will result in stronger exciton-plasmon coupling and larger Purcell factors.

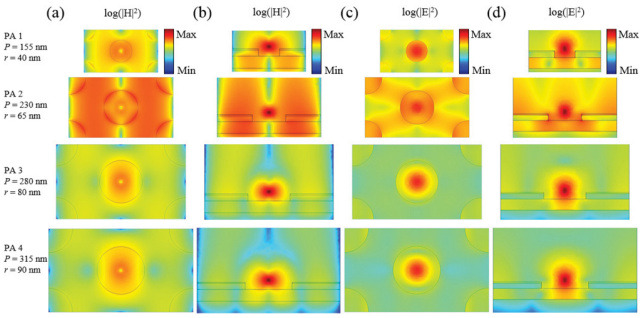

FIG. 5. Top (a) and side (b) views of magnetic field intensity distribution excited by a z-polarized electric dipole emitter at 620 nm, located at the center of the hole and 10 nm above the surface of the four PAs. (c) and (d) show the top and side views of electric field intensity distribution.

We have experimentally demonstrated the enhancement of CdSe/ZnS QDs' spontaneous emission rates and photoluminescence intensity with metamaterial perfect absorbers, which consist of a hexagonal array of holes on Ag-SiO_2-Ag thin films through rational design and possess near-unity absorption at the QD emission wavelength. Numerical simulations of the emission rate and intensity enhancement on the four studied QD-PA devices, as well as the electromagnetic field distribution under dipole emitter excitation, have been conducted to assist the comprehensive understanding of the experimental observations. The enhanced plasmon-exciton couplings between the emitters and PA resonate modes provide the possibility of controlling the QD emission processes towards the useful applications in metamaterial PA-based light harvesting and emitting devices.

The authors thank Dr. Yichen Liang, Dr. Ling Li, and Dr. Fei Cheng for the useful discussion. The authors acknowledge the support from the National Science Foundation (Nos. ECCS-1653032 and DMR-1552871) and the Office of Naval Research (No. N00014-16-1-2408). This work was performed, in part, at the Center for Integrated Nanotechnologies, an Office of Science User Facility operated for the U.S. Department of Energy (DOE) Office of Science. Sandia National Laboratories is a multi-program laboratory managed and operated by Sandia Corporation, a wholly owned subsidiary of Lockheed Martin Corporation, for the U.S. Department of Energy's National Nuclear Security Administration under Contract No. DE-AC04-94AL85000.

REFERENCES

[1] Y. Shirasaki, G. J. Supran, M. G. Bawendi, and V. Bulović, Nat. Photonics **7**(1), 13 (2013).
[2] A. J. Nozik, Physica E **14**(1–2), 115 (2002).
[3] I. Robel, V. Subramanian, M. Kuno, and P. V. Kamat, J. Am. Chem. Soc. **128**(7), 2385 (2006).
[4] G. Konstantatos, I. Howard, A. Fischer, S. Hoogland, J. Clifford, E. Klem, L. Levina, and E. H. Sargent, Nature **442**(7099), 180 (2006).
[5] S. Strauf, K. Hennessy, M. T. Rakher, Y.-S. Choi, A. Badolato, L. C. Andreani, E. L. Hu, P. M. Petroff, and D. Bouwmeester, Phys. Rev. Lett. **96**(12), 127404 (2006).
[6] P. Michler, A. Kiraz, C. Becher, W. V. Schoenfeld, P. M. Petroff, L. Zhang, E. Hu, and A. Imamoglu, Science **290**(5500), 2282 (2000).
[7] Y. Liang, W. Wang, J.-S. Moon, and J. G. Winiarz, Opt. Mater. **58**, 203 (2016).
[8] J.-S. Moon, Y. Liang, T. E. Stevens, T. C. Monson, D. L. Huber, B. D. Mahala, and J. G. Winiarz, J. Phys. Chem. C **119**(24), 13827 (2015).
[9] C. Cohen-Tannoudji, J. Dupont-Roc, and G. Grynberg, *Photons and Atoms—Introduction to Quantum Electrodynamics* (Wiley-VCH, 1997), p. 486.
[10] R. F. Oulton, V. J. Sorger, T. Zentgraf, R.-M. Ma, C. Gladden, L. Dai, G. Bartal, and X. Zhang, Nature **461**(7264), 629 (2009).
[11] E. M. Purcell, H. C. Torrey, and R. V. Pound, Phys. Rev. **69**(1–2), 37 (1946).
[12] M. Toishi, D. Englund, A. Faraon, and J. Vučković, Opt. Express **17**(17), 14618 (2009).
[13] X. Gan, Y. Gao, K. F. Mak, X. Yao, R.-J. Shiue, A. van der Zande, M. E. Trusheim, F. Hatami, T. F. Heinz, and J. Hone, Appl. Phys. Lett. **103**(18), 181119 (2013).
[14] K. J. Russell, T.-L. Liu, S. Cui, and E. L. Hu, Nat. Photonics **6**(7), 459 (2012).
[15] S. Noda, M. Fujita, and T. Asano, Nat. Photonics **1**(8), 449 (2007).

Published under license by AIP Publishing

[16]D. Englund, D. Fattal, E. Waks, G. Solomon, B. Zhang, T. Nakaoka, Y. Arakawa, Y. Yamamoto, and J. Vučković, Phys. Rev. Lett. **95**(1), 013904 (2005).
[17]P. Lodahl, S. Mahmoodian, and S. Stobbe, Rev. Mod. Phys. **87**(2), 347 (2015).
[18]A. Kinkhabwala, Z. Yu, S. Fan, Y. Avlasevich, K. Müllen, and W. E. Moerner, Nat. Photonics **3**(11), 654 (2009).
[19]V. Flauraud, R. Regmi, P. M. Winkler, D. T. L. Alexander, H. Rigneault, N. F. Van Hulst, M. F. García-Parajo, J. Wenger, and J. Brugger, Nano Lett. **17**(3), 1703 (2017).
[20]L. Li, W. Wang, T. S. Luk, X. Yang, and J. Gao, ACS Photonics **4**(3), 501 (2017).
[21]D. Lu, J. J. Kan, E. E. Fullerton, and Z. Liu, Nat. Nanotechnol. **9**(1), 48 (2014).
[22]H. N. S. Krishnamoorthy, Z. Jacob, E. Narimanov, I. Kretzschmar, and V. M. Menon, Science **336**(6078), 205 (2012).
[23]L. Sun, X. Yang, W. Wang, and J. Gao, J. Opt. **17**(3), 035101 (2015).
[24]H. A. Atwater and A. Polman, Nat. Mater. **9**(3), 205 (2010).
[25]M.-W. Tsai, T.-H. Chuang, C.-Y. Meng, Y.-T. Chang, and S.-C. Lee, Appl. Phys. Lett. **89**(17), 173116 (2006).
[26]N. Liu, M. Mesch, T. Weiss, M. Hentschel, and H. Giessen, Nano Lett. **10**(7), 2342 (2010).
[27]F. Cheng, X. Yang, and J. Gao, Opt. Lett. **39**(11), 3185 (2014).
[28]F. Cheng, X Yang, D. Rosenmann, L. Stan, D. Czaplewski, and J. Gao, Opt. Express **23**(19), 25329 (2015).
[29]Z. Li, W. Wang, D. Rosenmann, D. A. Czaplewski, X. Yang, and J. Gao, Opt. Express **24**(18), 20472 (2016).
[30]W. Wang, D. Rosenmann, D. A. Czaplewski, X. Yang, and J. Gao, Opt. Express **25**(17), 20454 (2017).
[31]F. Cheng, J. Gao, L. Stan, D. Rosenmann, D. Czaplewski, and X. Yang, Opt. Express **23**(11), 14552 (2015).
[32]Y. Cui, Y. He, Y Jin, F. Ding, L. Yang, Y. Ye, S. Zhong, Y. Lin, and S. He, Laser Photonics Rev. **8**(4), 495 (2014).
[33]Y. He, H. Deng, X. Jiao, S. He, J. Gao, and X. Yang, Opt. Lett. **38**(7), 1179 (2013).
[34]Y. Liang, J.-S. Moon, R. Mu, and J. G. Winiarz, J. Mater. Chem. C **3**(16), 4134 (2015).
[35]F. Cheng, J. Gao, T. S. Luk, and X. Yang, Sci. Rep. **5**, 11045 (2015).

Published under license by AIP Publishing